ELSEVIER

Journal of Atmospheric and Solar-Terrestrial Physics 67 (2005) 1744–1750

Journal of ATMOSPHERIC AND SOLAR-TERRESTRIAL PHYSICS

www.elsevier.com/locate/jastp

Submillimeter-wave and Hα observations of the event on 28 November, 2001

G. Cristiani[a,*], G. Martínez[a], C.H. Mandrini[a,1], C.G. Giménez de Castro[b], M.G. Rovira[a,1], P. Kaufmann[b,c], H. Levato[d,1]

[a]*Instituto de Astronomí a y Física del Espacio, CONICET-UBA, CC. 67 Suc. 28, 1428 Buenos Aires, Argentina*
[b]*Centro de Radio Astronomia e Astrofísica Mackenzie, Universidade Presbiteriana Mackenzie, Brazil*
[c]*CCS, Universidade Estadual de Campinas, Campinas, SP, Brazil*
[d]*Universidad Nacional de San Juan, San Juan, Argentina*

Available online 15 August 2005

Abstract

We present a detailed study of a 1B/M6.9 impulsive flare combining high time resolution (1 ms) and instantaneous emission source localization observations at submillimeter frequencies (212 GHz), obtained with the solar submillimeter telescope (SST), and Hα data from the Hα solar telescope for argentina (HASTA). The flare, starting at 16:34 UT, occurred in active region (AR) 9715 (NOAA number) on November 28, 2001, and was followed by an Hα surge. We complement our data with magnetograms from the Michelson Doppler Imager (SOHO/MDI). SST observed a short impulsive burst at 212 GHz, presenting a weak bulk emission (of about 90 sfu) composed of a few shorter duration (<5 s) structures. The integrated Hα and the 212 GHz light curves present a remarkable agreement during the impulsive phase of the event. The delay between both curves stays below 12 s (the time resolution of the Hα telescope). The flare as well as the surge are linked to new flux emergence very close to the main AR bipole. Taking into account the AR magnetic field evolution, we infer that magnetic field reconnection, occurring at low coronal levels, could have been at the origin of the flare; while in the case of surge this would happen at the chromospheric level.

Keywords: Sun: solar flares; Sun: chromosphere; Sun: magnetic field; Sun: radio emission

1. Introduction

Solar flares are rapid energy release transient phenomena that can be associated to the interaction of independent magnetic structures (see e.g. Mandrini et al., 1997, and references therein). Along the years, observational and theoretical evidences (Hachenberg and Wallis, 1961; Shimabukuro, 1970; Kaufmann et al., 1985; Ramaty and Manzhavizde, 1993) have shown that solar flares produce a large amount of non-thermal radiation in the millimetric/submillimetric range, as they do in hard X-rays. Analyzing flare emission at various wavelengths we can investigate the probable energy release mechanisms at work in flares and determine which are their main byproducts, in terms of particle acceleration and/or plasma heating.

Flare models consider that accelerated electrons emit gyroradiation in the millimetric/submillimetric radio range as they precipitate following magnetic loops (Dulk, 1985), and that the Hα emission starts rising

*Corresponding author. Tel.: +54 11 47832642; fax: +54 11 47868114.
E-mail address: gcristiani@iafe.uba.ar (G. Cristiani).
[1]Member of the Carrera del Investigador Científico, CONICET, Argentina.

1364-6826/$ - see front matter © 2005 Elsevier Ltd. All rights reserved.
doi:10.1016/j.jastp.2005.02.025

when the electrons reach the chromosphere. Both emissions begin almost simultaneously in models that consier that the energy released primarily accelerates particles (non-thermal flare models) and show delays of 10–20 s, depending on loop parameters, in models that propose that the energy released mainly heats the plasma (thermal flare models) (see Trottet et al., 2000, for details).

Chromospheric mass ejections, called surges, are a common phenomenon in ARs, especially when the region is flaring (for a study of the spatial distribution of surges and flares see e.g. Ögzüç et al., 1991). Hα surges have been studied for over 50 years (see Roy, 1973a,b). They are straight or slightly curved ejections that reach velocities of $50-200\,\mathrm{km\,s^{-1}}$ and heights of up to 200 Mm. After the ejection, the material is seen either to fade or to return to the chromosphere along the trajectory of ascent (Svestka, 1976; Tandberg-Hanssen, 1977; Foukal, 1990). The physical mechanisms involved in surges are not clearly understood. The surge may be driven by a high pressure gradient in a magnetic tube, as first proposed by Steinolfson et al. (1979) or it may be due to magnetic energy release through reconnection (Heyvaerts et al., 1977; Shibata et al., 1992). Kurokawa and Kawai (1993) showed that Hα surges are seen in the early stages of flux emergence, and concluded that they are produced by magnetic reconnection between the emerging flux region and the pre-existing surrounding field (see also Schmieder et al., 1996; Gaizauskas, 1996). Canfield et al. (1996) followed the same ideas to propose a phenomenological model to explain surges and X-ray jets in an AR.

In this paper, we present a detailed analysis of a 1B/M6.9 solar flare combining observations of two solar telescopes located in the Argentinean Andes, the solar submillimeter telescope (SST, Kaufmann et al., 2000) and the Hα telescope for Argentina (HASTA, Fernández Borda et al., 2002; Bagala et al., 1999). The flare occurred in AR 9715 on 28 November, 2001. It showed a very impulsive peak at ≈ 16:34 UT and consisted of two compact kernels. The SST data from this event have been analyzed in relation to a coronal mass ejection (CME) that was observed by the Large Angle Spectroscopic Coronagraph (SOHO/LASCO Brueckner et al., 1995) by Kaufmann et al. (2003). In this later paper, AR 9715 was proposed to be the source region of the CME. Furthermore, the SST observations were studied in connection with the occurrence of sub-second pulses, the origin of which still remains unknown, by Makhmutov et al. (2003). Six minutes after the main peak a chromospheric ejection became visible in the HASTA images. Both, the flare and the ejection, occurred in association with the emergence of new bipolar flux concentrations.

In Section 2, we present the observations included in the present study. We describe and analyze the magnetic field evolution in Section 2.1, the chromospheric data in Section 2.2 and the radio observations in Section 2.3. Finally, we discuss our results and conclude (Section 3).

2. Observations and data analysis

The event studied in this paper occurred in AR 9715 that was located at N04 E19 at 00:00 UT on November 28, 2001. During the period covered by our observations, several minor events were also observed in Hα in the same AR (some of them were classified as SF in solar geophysical data comprehensive reports, see http://sgd.ngdc.noaa.gov/sgd/jsp/solarindex.jsp). The Hα kernels of these events were almost cospatial with the kernels of the largest event (so, they were homologous), which is object of this work. In this section we present multiwavelength data to find clues about the origin of this flare.

2.1. The photospheric evolution

To study the dynamical behavior of the AR magnetic field, we have used full disk level 1.5 magnetograms obtained by MDI (Scherrer et al., 1995). These data are the average of 5 magnetograms with a cadence of 30 s. They are constructed once every 96 min. The error in the flux densities per pixel in the averaged magnetograms is ≈ 9 G, and each pixel has a mean area of $1.96\,\mathrm{Mm^2}$. We produced a magnetic field movie starting at the time the AR appeared at the eastern solar limb, and extending for seven days, that allowed us to identify the emergence of several new flux concentrations.

Fig. 1 shows the line of sight magnetic field at different stages of the AR evolution. AR 9715 was mainly bipolar when it appeared on the eastern solar limb (polarities are numbered as 1 and 2 in Fig. 1). As the two main polarities started diffusing, new bipoles emerged both at the eastern portion of the AR and at its western portion. A new emerging bipole can be seen in the central panel of Fig. 1 (the polarities are numbered as 3 and 4 and they are first visible in MDI map at 9:35 UT on 27 November). The interaction of this eastern bipole with the surrounding AR field can beat the origin of four plage enhancements which were present all along our Hα observations (see Fig. 3a).

Two other bipoles appeared at the western portion of the AR. One of them emerged very close to the preceding polarity of AR 9715 (polarities 5 and 6 in Fig. 1, they are first visible in MDI map at 16:03 UT on 27 November). In particular, its positive polarity merged with the northern portion of the main positive AR field (see next paragraph), while its negative polarity was cancelling partly with the main positive flux (see bottom panel in Fig. 1). The second bipole had a weaker field (polarities 7 and 8 in Fig. 1, they are first visible in MDI

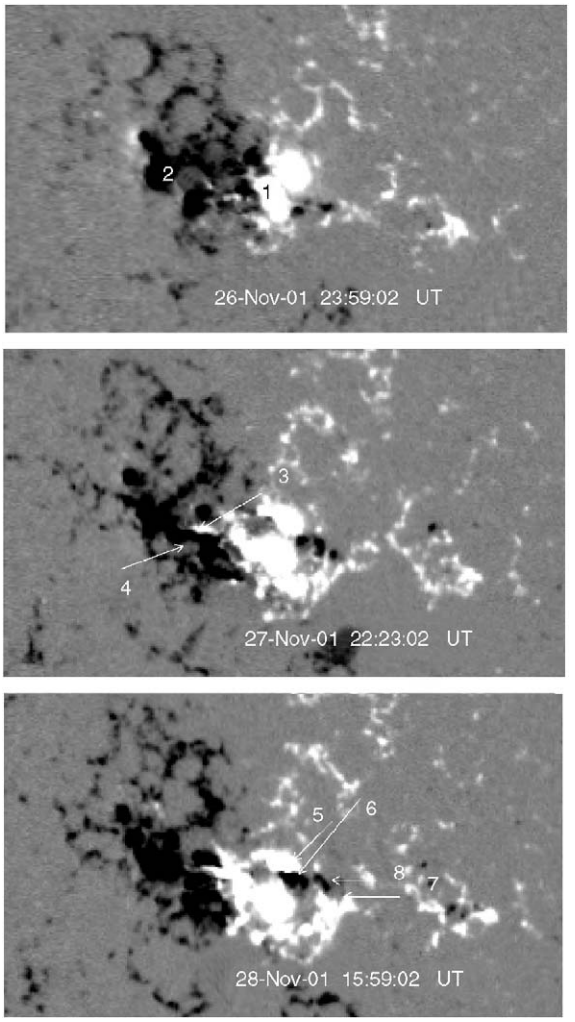

Fig. 1. The photospheric line of sight component of the magnetic field in AR 9715 from November 26 to November 28, 2001. Sections of MDI full disk observations covering an area of 267 pixels × 156 pixels (1 pixel ≈ 1.96 arcsec). North is up and West is to the right in this and following figures. The data represented in grey scale are saturated above (below) 200 G (−200 G). The numbers refer to the polarities of different emerging bipoles in the AR (see text).

map at 19:11 UT on 27 November). The interaction of these two bipoles with the pre-existing AR field could have been at the origin of the flare and the following surge. As the AR evolved, polarities 5 and 6 were seen to decay (by November 30) simultaneously, indicating that they probably belonged to the same emerging flux tube.

Fig. 2 shows the evolution of the magnetic flux corresponding to polarity 5 and polarities 6 and 8 added together (since we cannot separate precisely the pixels belonging to each of them). The curves are computed including pixels where the absolute value of the magnetic

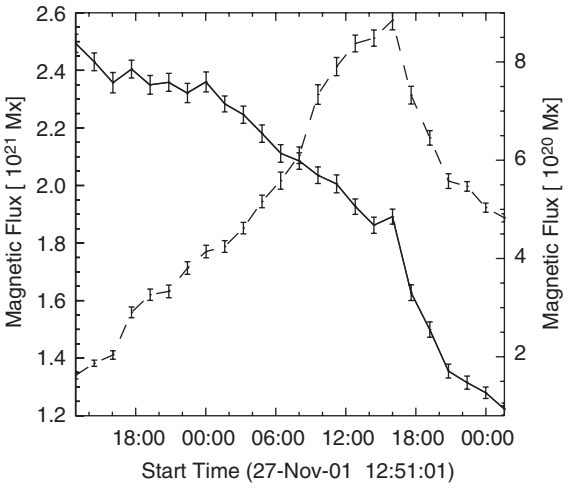

Fig. 2. Magnetic flux evolution for some polarities in AR 9715. The continuous curve corresponds to the positive polarity 5, this polarity merges with the already decaying polarity 1 (see text for an explanation). The dashed curve shows the evolution of the absolute flux value for the negative polarities 6 and 8 added up together. The error bars have been estimated considering MDI error in the flux densities per pixel. The left (right) vertical axis corresponds to the positive (negative) polarities. Notice the different vertical scales.

field is above 10 G. The negative flux increases monotonically from its appearance and reaches maximum at 15:59 UT on 28 November, which is the magnetic map closest to the starting time of the events analyzed here. After this maximum, it decreases monotonically. The behavior of the positive flux curve is more complicated. We observe a global decaying evolution; however, this curve shows a local maximum at the same time the negative flux curve reaches its absolute maximum value. This is the behavior we expect if polarity 5 emerges by the already decaying polarity 1 and merges with it.

2.2. The chromospheric evolution

The Hα observations were carried out with the HASTA instrument. HASTA is located at the Estación de Altura Ulrico Cesco of OAFA (Observatorio Astronómico Félix Aguilar), El Leoncito, San Juan, Argentina. A tunable Lyot-Öhmann filter (0.03 nm bandpass) and a digital CCD-camera were installed at the focus of the telescope with a focal length of 1.65 m and a free aperture of 0.11 m. The CCD-camera has 1280 × 1024 pixels that cover 2.07 arcsec on the Sun. The instrument works in two different modes: the patrol mode and the flare mode. In the patrol mode, HASTA takes full-disk images every 2 min. When a solar flare is detected, HASTA switches to the flare mode. In the flare mode, HASTA takes full-disk images every 10 s approximately.

On November 28, 2001, HASTA observations covered the period from 11:12 UT to 21:58 UT. During this period AR 9715 displayed different levels of activity, as discussed above.

All along our Hα observations two intense kernels were observed overlaying polarities 1 and 6. The intensity in these kernels was always higher than the intensity in the four eastern kernels (see Fig. 3a). The two western kernels reach their highest intensity values during the flare at 16:34 UT (see Fig. 3b). As the flare evolved, the Hα brightenings elongated towards the West overlaying polarities 7 (at its northern portion), part of 8 and of the positive small flux concentration to the West of 5. The error in the overlay between HASTA and MDI stays within ±1 HASTA pixel.

In Fig. 4 we depict the Hα lightcurve adding up the intensity in the two most intense kernels. We remark that the curves for the individual kernels show an excellent agreement.

At around 16:42 UT (see Fig. 3c), dark chromospheric material was clearly observed in HASTA images ejected towards the North–West. We cannot ascertain the time at which the ejection initiated since the flare brightness dominated our Hα images. The surge started to be observed by the end time of the light curves depicted in Fig. 4 (top). Taking into account the surges line of sight velocity range (see references in the Introduction), the extension of this surge in the Hα image at 16:42:54 UT ($\approx 3 \times 10^4$ km) and assuming that the velocity range is also valid for the surge projection on the solar disk, we can estimate the starting time for the surge by backwards extrapolation. We find that the surge could have started between ≈ 16:34 UT (so, by the flare starting time) and ≈ 16:40 UT. From the coalignment of MDI and HASTA, the base of the ejection laid on polarity 7 (see Fig. 3). The material had a curved downward shape and could be followed in HASTA images until ≈ 17:00 UT.

2.3. The radio emission

The SST (Kaufmann et al., 2001) provides observations at 212 and 405 GHz with a time resolution of 1 ms at that time. The multiple receiver focal array produces six beams (1–4 at 212 GHz and 5–6 at 405 GHz). A cluster of three beams (2–4) overlapping at ~ half power

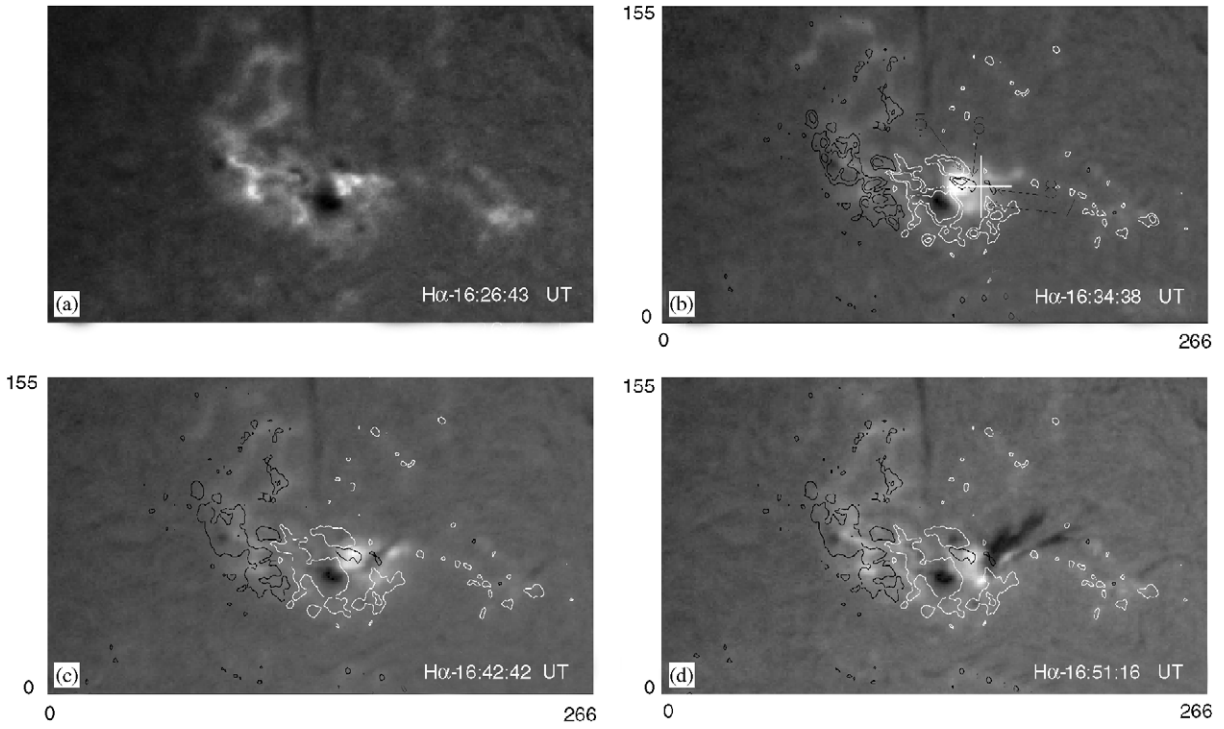

Fig. 3. The chromospheric evolution as seen by HASTA on 28 November, 2001. The panels depict portions of HASTA full disk data centered in AR 9715, overlaid with MDI isocontours (except in (a)), where we have not included them to avoid covering the plage brightenings towards the East. Two isocontours (±200., 500. G) of MDI at 15:59 UT (see Fig. 1), positive (negative) values drawn in white (black), are shown in (b); while only one (±200. G) is depicted in (c) and (d). The location of the SST submillimeter source, computed as discussed in Section 2.3, is also marked in (b), the error (≈ 30 arcsec) in the determination of the source position is indicated by the cross size. The area covered by the panels is 257 × 150 pixels (1 pixel ≈ 2.07 arcsec).

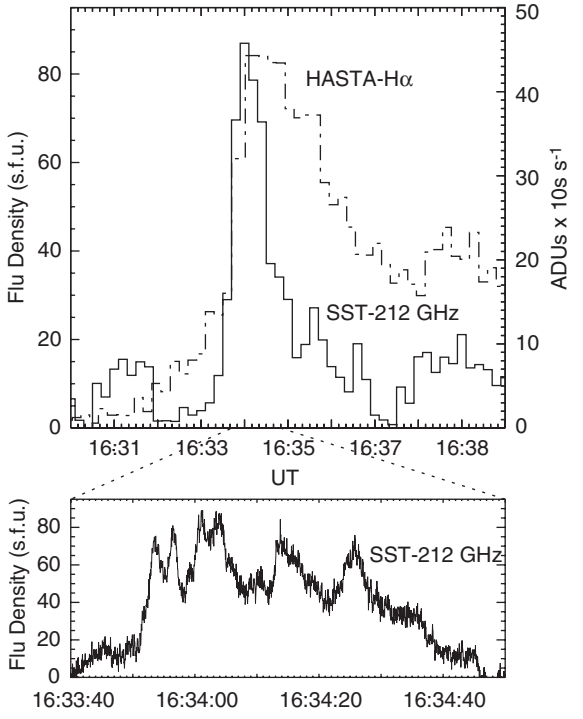

Fig. 4. A comparison of the Hα and submillimeter lightcurves (shown as histograms). The top image corresponds to the SST lightcurve (1 ms temporal resolution), averaged so as to adjust to the Hα temporal resolution (12 s), together with the one in Hα. The vertical left axis corresponds to SST observations, while the right one to the HASTA data (where ADUs means analogue-to-digital conversion units). The bottom figure is a zoom of SST observations between 16:33:40 UT and 16:34:50 UT averaged every 40 ms.

beam width (HPBW ~4′) allows us to estimate, at each time, the location of the centroid of emission for a small (compared to HPBW) emitting source, which is used subsequently to compute the source flux density (Giménez de Castro et al., 1999). The flux at 405 GHz is derived assuming the 212 GHz source positions.

During November 28, 2001, at the flare time the projection on the sky of beam 5 was centered on and tracking AR 9715, while those of beams 2–4 varied with time but always covered the active region. Beam 1 was located on the quiet Sun far away from AR 9715 and beam 6 was inactive. During the observations we had very good atmospheric conditions. The atmospheric zenith opacities were estimated to be ~0.14 and ~0.70 nepers at 212 and 405 GHz, respectively, and were used to correct for atmospheric attenuation.

To minimize the atmospheric influence in the data we use the beam-switching technique, subtracting the signal from beam 1 (which was pointing to the quiet Sun) from those of beams 2, 3 and 4. In this way, we also remove the contribution of the quiet Sun that, at a given frequency, is expected to be similar in the different beams, and we can better determine the pre-flare level. For this particular event, it was not possible to use this technique with the data in 405 GHz because channel 6 was inactive. Taking into account the uncertainties in the determination of the different parameters (antenna temperature calibration, aperture efficiencies, beams form and position, etc.) a reasonable value for relative uncertainties in the calculated flux density at 212 GHz is ±30%.

Fig. 4 top panel depicts the SST 212 GHz time profile together with the Hα light curve. The SST data have been averaged in order to match the temporal resolution of the Hα data (12 s). At the flare impulsive phase, both curves are seen to evolve with a remarkable agreement. We found that within the time interval 16:33:40 UT–16:34:10 UT (during which the maximum is achieved in both wavelengths) the rising slope was the same.

The radio burst exhibits a structured shape (see bottom panel of Fig. 4) presenting five pulses with durations in the range of 1–5 s. Pulse separations stayed below 12 s, the temporal resolution of the Hα telescope so they cannot be resolved in the Hα intensity curve. For each of these peaks we determined the position of the source (centroid of the emission), so we had five source locations on the solar disk. The sources show a very compact structure, with a dispersion in their positions of the order of 10 arcsec. This is an indication of a single source, but using only SST observations we cannot rule out the possibility of several very compact and near sources. In Fig. 3b the location of the source observed at 212 GHz has been overlaid to the Hα image at ≈ 16:34 UT, the size of the cross indicates the error in the source localization. Notice that both HASTA kernels lie at the same location of the SST centroid of emission, within errors.

As we did not observe any significant radio emission above noise level at 405 GHz during the impulsive flare phase (that we define as the duration of the 212 GHz peak in Fig. 4), we adopted a value of 24 s.f.u., the flux density standard deviation in this range, as an upper bound for the emission.

3. Discussion and conclusions

We have analyzed multiwavelength observations of a 1B/M6.9 flare that occurred on November 28, 2001. The flare presented an impulsive peak in submillimeter waves (212 GHz) at 16:34 UT. The emission in this wavelength showed a remarkable agreement in rising time with the emission in Hα that came from the two flare kernels. The two flare kernels were located at both sides of the neutral line separating polarities 1 and 6 (1 belonging to the original AR bipole and 6 belonging to a new bipole emerging during November 27). These kernels were very

compact and were not seen to move away from the neutral line as it happens in a typical two-ribbon flare. Furthermore, Hα compact brightenings were seen located at the same place of the flare kernels in HASTA data from the beginning of our observational period.

As the flare evolved, the flare kernels elongated towards the West overlaying polarities 7 and 8. At that stage, after the steep submillimeter peak and during the decay phase of the Hα emission, a chromospheric surge became visible in HASTA images at ≈16:42 UT, though it probably started before that time, as discussed in Section 2.2. The base of the surge was located on polarity 7.

Taking into account the magnetic field evolution and the location of flare kernels, we may conclude that the flare was the result of the interaction, via magnetic field reconnection, of newly emerged bipoles with the pre-existing AR magnetic field (see several examples based on magnetic field topology analysis in Démoulin et al., 1997; Mandrini et al., 1997). For the two Hα flare kernels located on 1 and 6, magnetic reconnection occurred between field lines anchored in bipole 5–6 with field lines anchored in 1. This process started much before the flare impulsive phase as confirmed by the presence of Hα brightenings at the same location, and the fact that bipole 5–6 started to emerge on November 27, 2001, at 16:03 UT. As more flux was brought up by emergence (see the magnetic flux evolution in Fig. 2) against the pre-existing field, the flare occurs. The emergence of a new photospheric bipole against an overlying magnetic field does not imply that a flare will occur immediately, critical conditions have to be achieved (e.g. development of turbulence in the current sheet, when it reaches a critical height, formed between the emerging flux and the overlaying field, was proposed by Heyvaerts et al., 1977, in their classical flux emergence model).

The flare kernels are at the base of newly reconnected magnetic loops (see the previously mentioned references); then, the spatial separation of the kernels is related to the height of the reconnecting region. Due to the closeness of the flare kernels to the magnetic field inversion line (≈5 Mm, measured on an overlay of an HASTA image at ≈16:33 UT and the closest MDI magnetogram), we can conclude that the reconnection process occurs at low heights in the atmosphere (≈5 Mm, assuming semicircular loop shapes). From the FAL atmospheric models (Fontenla et al., 1990) this locates the reconnection site at the base of the corona, but above the chromosphere and the transition region. Because of the large gravitational scale height of the corona (≈50−100 Mm), the plasma density in the pre-reconnected loops is expected to be comparable to the density at larger heights (few 10 Mm).

The origin of surges has been in general associated with magnetic reconnection between a new emerging flux region and the pre-existing magnetic field (see references in Section 1), and this seems to be the case in the example analyzed here. That is to say, a process similar to the one described above, but now occurring between field lines anchored in bipole 7–8 and field lines anchored in the remaining northern portion of 1, can give rise to the surge and consequent brightenings observed during the decay phase of the flare. Since the reconnection process has to bring up chromospheric material, in this case it occurs at low atmospheric heights, probably the upper chromosphere (see an example based on magnetic field topology analysis in which the reconnection process occurs at separatrices associated with field lines which are tangent to the photosphere, namely 'bald patches', and originate a surge in Mandrini et al., 2002). Magnetic reconnection is presently known to be fast enough at photospheric and chromospheric levels. The faster tearing mode grows with a time scale between 6 and 20 s (Sturrock, 1999) and the Sweet–Parker model is fast enough to explain the observed flux cancellation rate in ARs (Litvinenko and Martin, 1999).

The flux density at 405 GHz with an upper bound limit of about 24 s.f.u. implies that the radio emission cannot have a thermal Bremsstrahlung origin. With a maximum value of about 90 s.f.u. at 212 GHz, the spectrum between 212 and 405 GHz has a power law index $\leqslant -1.9$, which cannot be in anyway representative of free–free emission. We found a striking coincidence in the rising time between SST and HASTA lightcurves (within HASTA temporal resolution) during the impulsive phase of the flare. HASTA temporal resolution is rather low and does not let us discriminate between different energy transport processes (i.e. accelerated particle or conduction fronts). In this sense, the upgrade of the HASTA telescope, which is planned in the near future, will allow a high cadence image acquisition ($\geqslant$20 frames/s). This will be an important step to bring light on this central question.

Acknowledgements

We thank Dr. P. Démoulin for a critical reading of this article. This research was funded by the Brazilian research agency Fundaçao de Amparo a Pesquisa do Estado de São Paulo Grant no. 99/01626-7 and by the Argentinean Grants UBACyT X329, CONICET PIP-2388 and ANPCYT PICT-12187. The authors thank the SoHO/MDI consortium for MDI data. SoHO is a joint project by ESA and NASA.

References

Bagalá, L.G., Bauer, O.H., Fernández Borda, R., Francile, C., Haerendel, G., Rieger, R., Rovira, M.G., 1999. The New

Hα Solar Telescope at the German–Argentinian Solar Observatory. ESA SP 448, 469–474.

Brueckner, G.E., Howard, R.A., Koomen, M.J., Korendyke, C.M., Michels, D.J., Moses, J.D., Socker, D.G., Dere, K.P., Lamy, P.L., Llebaria, A., Bout, M.V., Schwenn, R., Simnett, G.M., Bedford, D.K., Eyles, C.J., 1995. The Large Angle Spectroscopic Coronagraph (LASCO). Solar Physics 162, 357–402.

Canfield, R.C., Reardon, K.P., Leka, K.D., Shibata, K., Yokohama, T., Shimojo, M., 1996. Hα surges and X-ray jets in AR 7260. Astrophysical Journal 464, 1016–1029.

Démoulin, P., Bagalá, L.G., Mandrini, C.H., Henoux, J.C., Rovira, M.G., 1997. Quasi-separatrix layers in solar flares. II. Observed magnetic configurations. Astronomy and Astrophysics 325, 305–317.

Dulk, G.A., 1985. Radio emission from the sun and stars. Annual Review of Astronomy and Astrophysics 23, 169–224.

Fernández Borda, R., Mininni, P., Mandrini, C.H., Gómez, D.O., Bauer, O., Rovira, M.G., 2002. Automatic solar flare detection using neural network techniques. Solar Physics 206, 347–357.

Fontenla, J.M., Avrett, E.H., Loeser, R., 1990. Energy balance in the solar transition region I—hydrostatic thermal models with ambipolar diffusion. Astrophysical Journal 355, 700–718.

Foukal, P., 1990. Solar Astrophysics. Wiley, New York, 354.

Gaizauskas, V., 1996. Magnetic reconnection as a driver of chromospheric surges. Solar Physics 169 (Issue 2), 357–366.

Giménez de Castro, C.G., Raulin, J.-P., Makhmutov, V.S., Kaufmann, P., Costa, J.E.R., 1999. Instantaneous positions of microwave solar bursts: properties and validity of the multiple beam observations. Astronomy and Astrophysics Supplement Series 140, 373–382.

Hachenberg, O., Wallis, G., 1961. Das Spektrum der Bursts der Radiofrekuenzstrahlung der Sonne in cm—Wellenbereich. Zeitschrift für Astrophysyk 52, 42–72.

Heyvaerts, J., Priest, E.R., Rust, D.M., 1977. An emerging flux model for the solar flare phenomenon. Astrophysical Journal 216, 123–137.

Kaufmann, P., Correia, E., Costa, J.E.R., Zodi Vaz, A.M., Dennis, B.R., 1985. Solar burst with millimetre-wave emission at high frequency only. Nature 313, 380–382.

Kaufmann, P., Costa, J.E.R., Giménez de Castro, C.G., Hadano, Y.S., Kingsley, J.S., Kingsley, R.K., Levato, H., Marún, A., Raulin, J.-P., Rovira, M.G., Correia, E., Silva, A.V.R., 2000, In: Proceedings of SBMO/IEEE MTT—S International Microwave and Optoelectronics Conference, 439–442.

Kaufmann, P., Raulin, J.-P., Correia, E., Costa, J.E.R., Giménez de Castro, C.G., Silva, A.V.R., Levato, H., Rovira, M.G., Mandrini, C.H., Fernández Borda, R., Bauer, O., 2001. Solar flare observations at submmillimeter-waves. In: Pål Brekke, Bernhard Fleck, Joseph B. Gurman (Eds.), Proceedings of IAU Symposium 203, 2001, p. 283.

Kaufmann, P., Giménez de Castro, C.G., Makhmutov, V.S., Raulin, J.-P., Schwenn, R., Levato, H., Rovira, M.G., 2003. Launch of solar coronal mass ejections and submillimeter pulse bursts. Journal of Geophysical Research 108, 1280–1295.

Kurokawa, H., Kawai, G., 1993. Hα surge activity at the first stage of magnetic flux emergence. In: Zirin, H., Ai, G., Wang, H. (Eds.), The Magnetic and Velocity Fields of Solar Active Regions ASP Conference Series, vol. 46, pp. 507–510.

Litvinenko, Y.E., Martin, S.F., 1999. Magnetic reconnection as the cause of a photospheric cancelling feature and mass flows in a filament. Solar Physics 190, 45–58.

Makhmutov, V.S., Raulin, J.-P., Giménez de Castro, C.G., Kaufmann, P., Correia, E., 2003. Wavelet decomposition of submillimeter solar radio bursts. Solar Physics 218, 211–220.

Mandrini, C.H., Démoulin, P., Bagalá, L.G., van Driel-Gesztelyi, L., Hénoux, J.C., Schmieder, B., Rovira, M.G., 1997. Evidence of magnetic reconnection from Hα, soft X-ray and photospheric magnetic field observation. Solar Physics 174, 229–240.

Mandrini, C.H., Démoulin, P., Schmieder, B., Deng, Y.Y., Rudawy, P., 2002. The role of magnetic bald patches in surges and arch filament systems. Astronomy and Astrophysics 391, 317–329.

Özgüç, A., Yeşilyaprak, H., Düzgelen, A., 1991. Distribution of solar surges. Astronomy and Astrophysics 241, 209–211.

Ramaty, R., Manzhavizde, N., 1993. Theoretical models for high-energy solar flare emissions. In: Ryan, J., Vestrand, W.T. (Eds.), High-Energy Solar Phenomena—a New Era of Spacecrafts Measurements, AIP Conference Proceedings, vol. 294, pp. 26–44.

Roy, J.-R., 1973a. The magnetic properties of solar surges. Solar Physics 28, 95–114.

Roy, J.-R., 1973b. The dynamics of solar surges. Solar Physics 32, 139–151.

Scherrer, P.H., Bogart, R.S., Bush, R.I., et al., 1995. The Solar Oscillations Investigation-Michelson Doppler Imager. Solar Physics 162, 129–188.

Schmieder, B., Rovira, M., Simnett, G.M., Fontenla, J.M., Tandberg-Hanssen, E., 1996. Subflares and surges in AR 2744 during the Solar Maximum Mission. Astronomy and Astrophysics 308, 957–969.

Shibata, K., Nozawa, S., Matsumoto, R., 1992. Magnetic reconnection associated with emerging magnetic flux. Astronomical Society of Japan Publications 44, 265–272.

Shimabukuro, F.I., 1970. The observation of 3.3-mm burst and their correlation whit soft X-ray burst. Solar Physics 15, 424–432.

Steinolfson, R.S., Schmahl, E.J., Wu, S.T., 1979. Hydrodynamic simulations of flare/surge events. Solar Physics 63, 187–200.

Sturrock, P.A., 1999. Chromospheric magnetic reconnection and its possible relationship to coronal heating. Astrophysical Journal 521, 451–459.

Svestka, Z., 1976. Solar Flares. Reidel, Dordrecht.

Tandberg-Hanssen, E., 1977. Prominences. In: Bruzek, A., Durrant, C.J. (Eds.), Illustrated Glossary of Solar and Solar Terrestrial Physics. Dordrecht, Reidel, p. 106.

Trottet, G., Rolli, E., Magun, A., Barat, C., Kuznetsov, A., Sunyaev, R., Terhekov, O., 2000. The fast and slow chromospheric responses to non thermal particles produced during the 1991 March 13 hard X-ray/gamma-ray flare at ~08 UTC. Astronomy and Astrophysics 356, 1067–1075.